Exploring the radio and GeV-TeV γ-ray connection in the different blazar sub-classes

R. Lico[1,2], M. Giroletti[2], M. Orienti[2,3], L. Costamante[4], V. Pavlidou[5], F. D'Ammando[2] and F. Tavecchio[6]

[1]Max-Planck-Institut für Radioastronomie, Auf dem Hügel, 69, D-53121 Bonn, Germany.
email: rlico@mpifr-bonn.mpg.de

[2]INAF - Istituto di Radioastronomia, via Gobetti 101, 40129 Bologna, Italy.

[3]DIFA, Università di Bologna, via Gobetti 93/3, 40129 Bologna, Italy.

[4]ASI Unità Ricerca Scientifica, Via del Politecnico snc, I-00133, Roma, Italy.

[5]Department of Physics and Institute for Plasma Physics, University of Crete, 71003 Heraklion, Greece.

[6]INAF Osservatorio Astronomico di Brera, via E. Bianchi 46, I-23807 Merate, Italy.

Abstract. As revealed by the *Fermi*-LAT, blazars represent the dominant population of γ-ray emitters. An essential step for understanding blazar physics and the emission mechanisms is the investigation of a possible connection between the observed low- and high-energy emission. A number of works report on the existence of a significant correlation between radio emission and 0.1-100 GeV γ rays. How does this correlation evolve when very high energy (VHE, $E > 0.1$ TeV) γ rays are considered? The possible radio-VHE emission connection is still elusive mainly because of the lack of a homogeneous VHE sky coverage. In this work we explore the connection between the parsec-scale radio emission and GeV-TeV γ rays by using two unbiased blazar samples extracted from the 1FHL ($E > 10$ GeV) and 2FHL ($E > 50$ GeV) *Fermi* catalogs. For comparison, we perform the same analysis by using the 3FGL 0.1-300 GeV γ-ray energy flux. Overall, we find out that there is no significant connection between radio and γ-ray emission above 10 GeV for all the blazar sub-classes with the exception of high synchrotron peaked objects. Conversely, when 0.1-300 GeV γ-ray energies are considered, a strong and significant correlation is found for all of the blazar sub-classes. We interpret these results within the context of the blazar spectral energy distribution properties.

Keywords. Galaxies: active - Gamma rays: galaxies - Radio continuum: galaxies – BL Lacertae objects: general – (Galaxies:) quasars: general – Galaxies: statistics

1. Introduction

Among active galactic nuclei (AGNs) blazars represent the most extreme objects. The blazar spectral energy distribution (SED) is dominated by two distinctive non-thermal components: a low-frequency component produced by synchrotron emission from relativistic electrons within the jet, peaking from radio to soft X-ray energies, and a high-frequency component, peaking from X-ray to γ-ray bands, commonly though to be produced by inverse Compton (IC) scattering of low energy photons by relativistic electrons in the jet. For the high-energy emission we invoke the synchrotron-self-Compton (e.g. Maraschi *et al.* 1992) or the external Compton (e.g. Ghisellini & Madau 1996) emission mechanisms when the scattered low-energy photons are the same photons produced by the synchrotron or external photons, respectively. According to the position of the synchrotron component peak $\nu_{\rm peak}^{\rm Syn}$ in the SED, blazars are classified as low-synchrotron peaked (LSP) or high-synchrotron peaked (HSP) whether $\nu_{\rm peak}^{\rm Syn}$ is $< 10^{14}$ Hz or $> 10^{15}$ Hz,

respectively. Blazars with $10^{14}\,\mathrm{Hz} < \nu_{\mathrm{peak}}^{\mathrm{Syn}} < 10^{15}\,\mathrm{Hz}$ are classified as intermediate synchrotron peaked (ISP). Blazars are also classified into flat spectrum radio quasars (FSRQs) and BL Lac objects (BL Lacs) according to the presence or not of broad emission lines in their optical spectra (e.g. Stickel *et al.* 1991). In general FSRQs are of LSP type, while BL Lacs can be part of all three classes.

After the large area telescope (LAT), launched in 2008 onboard the *Fermi* satellite, clearly showed that blazars dominate the census of the γ-ray sky (e.g. Acero *et al.* 2015), many efforts were made for the investigation of the possible radio and γ-ray emission up to 100 GeV connection (e.g. Kovalev *et al.* 2009; Giroletti *et al.* 2010; Ackermann *et al.* 2011). In particular, it was found that the correlation strength becomes weaker when higher γ-ray energies are considered (e.g. Ackermann *et al.* 2011; Piner & Edwards 2014; Mufakharov *et al.* 2015). However, owing to the lack of a homogeneous coverage of the very high energy (VHE, $E > 0.1\,\mathrm{TeV}$) sky, due to the limited operational mode of the imaging atmospheric Cherenkov telescopes, the possible connection between radio and VHE emission connection is still elusive.

In Lico *et al.* (2017), we investigate the connection between very long baseline interferometry (VLBI) radio emission and GeV/TeV γ rays by using two large and unbiased samples blazars from the 1FHL ($E > 10\,\mathrm{GeV}$, Ackermann *et al.* 2013) and 2FHL ($E > 50\,\mathrm{Gev}$, Ackermann *et al.* 2016) *Fermi* catalogs. In this proceeding we briefly report and summarize some results obtained for the 1FHL blazar sample.

2. Results and discussion

To understand blazar physics and to discern among the various emission models, the investigation of a possible connection between low- and high-energy connection represents a fundamental step. A significant correlation between radio and 0.1-100 GeV γ-ray emission was found in previous studies (e.g. Ghirlanda *et al.* 2010; Ackermann *et al.* 2011). In this work we investigate how this correlation evolves at higher γ-ray energies. For our analysis we use a sample of 237 blazars for which we both consider the 1FHL (10-500 GeV) and 3FGL (0.1-300 GeV, Acero *et al.* 2015) γ-ray energy ranges. At radio frequencies we use 8 GHz VLBI flux densities from the radio fundamental catalog (http://astrogeo.org/rfc/). For more details on the sample selection see Lico *et al.* (2017).

The scatter plots of the VLBI flux density versus 1FHL and 3FGL γ-ray energy flux for the various blazar sub-classes (BL Lac, FSRQ, HSP, ISP, and LSP) are shown in Fig. 1 (top and bottom panels, respectively). The scatter plots for the full sample are reported in Fig. 2 for both the $E > 10\,\mathrm{GeV}$ 1FHL (left frame) and $E > 0.1\,\mathrm{GeV}$ 3FGL (right frame) energy fluxes. Red, green and blue colors represent LSPs, ISPs and HSPs, respectively. Filled and empty symbols represent those sources with known and unknown redshift, and in black color are indicated those blazars without any spectral classification. The results of our analysis, for which we use the statistical method proposed by Pavlidou *et al.* 2012 that takes into account both the various observational biases and the distance effects, are shown in Table 1. A statistically significant correlation ($r > 0.7$ with $p < 10^{-6}$) is found for the full sample and for each single blazar sub-class when 0.1-300 GeV γ rays from the 3FGL catalog are considered. On the other hand, when 10-500 GeV 1FHL γ-ray energy fluxes are considered the correlation breaks for all of the blazar sub-classes except for HSP objects ($r > 0.6$ with $p < 10^{-6}$). Similar results are obtained for the 2FHL ($E > 50\,\mathrm{GeV}$) blazar sample (see Lico *et al.* 2017).

To explain this correlation behavior we investigate the SED properties for the different blazar sub-classes. A simplified sketch of LSP, ISP and HSP (top, middle and bottom curve, respectively) SEDs is reported in Fig. 3, where the 0.1-300 GeV 3FGL energy range is represented by the green area, and the 1FHL ($E > 10\,\mathrm{GeV}$) and 2FHL ($E > 50\,\mathrm{GeV}$) energy thresholds are represented by the vertical dotted and dash-dotted vertical lines,

Table 1. Correlation analysis results. col(1): sub-classes; col(2): source catalog; col(3): number of sources in each subset; col(4): number of redshift bins (each bin contains > 10 objects); col (5): Pearson correlation coefficient (r); col (6): statistical significance (p).

Source type	Catalog	Number of sources	Number of z-bins	r-Pearson	Significance
All sources	1FHL	147	14	-0.05	0.59
	3FGL	147	14	0.71	$< 10^{-6}$
BL Lac	1FHL	100	9	0.12	0.55
	3FGL	100	9	0.70	$< 10^{-6}$
FSRQ	1FHL	44	4	-0.01	0.99
	3FGL	44	4	0.49	$< 10^{-6}$
HSP	1FHL	60	5	0.57	1.0×10^{-6}
	3FGL	60	5	0.77	$< 10^{-6}$
ISP	1FHL	23	2	0.19	0.40
	3FGL	23	2	0.46	2.5×10^{-2}
LSP	1FHL	52	5	0.21	0.12
	3FGL	52	5	0.43	3.0×10^{-6}
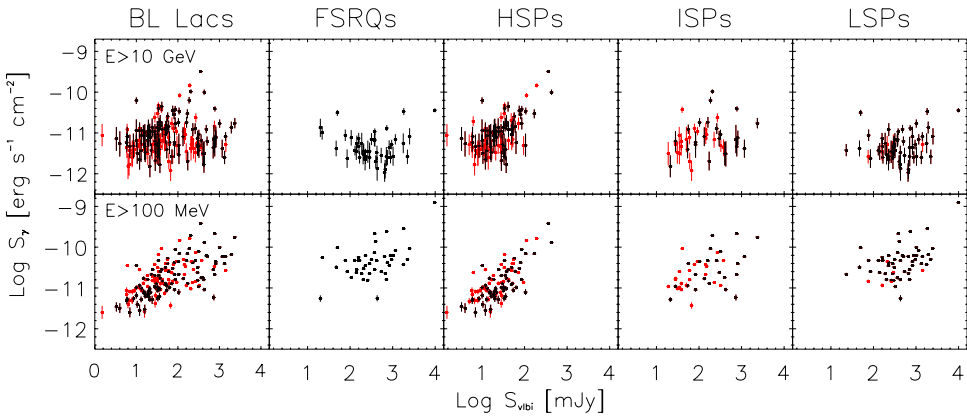
Figure 1. Scatter plot of the VLBI radio emission and 1FHL (upper frames) and 3FGL (lower frames) energy flux the different sub-classes (BL Lacs, FSRQs, HSPs, ISPs, and LSPs). The black and red colors represent sources with or without redshift, respectively.
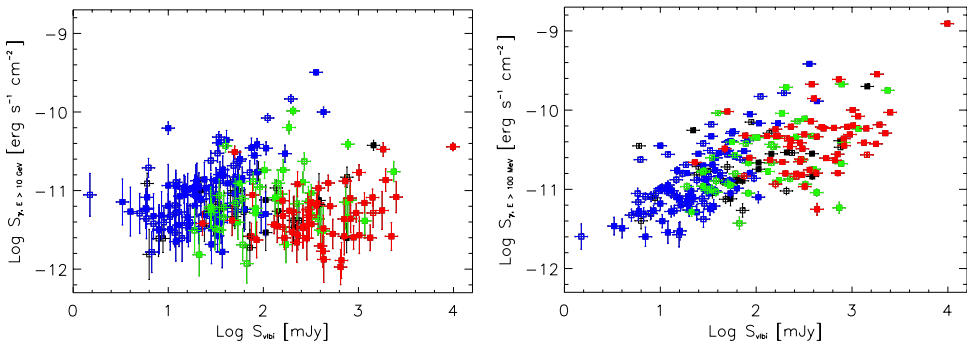
Figure 2. Full sample VLBI radio versus 1FHL (left frame) and 3FGL (right frame) energy flux scatter plots. Red, green and blue colors represent LSPs, ISPs and HSPs, respectively. Filled and empty symbols represent those sources with known and unknown redshift, and in black color are indicated those blazars without any spectral classification.
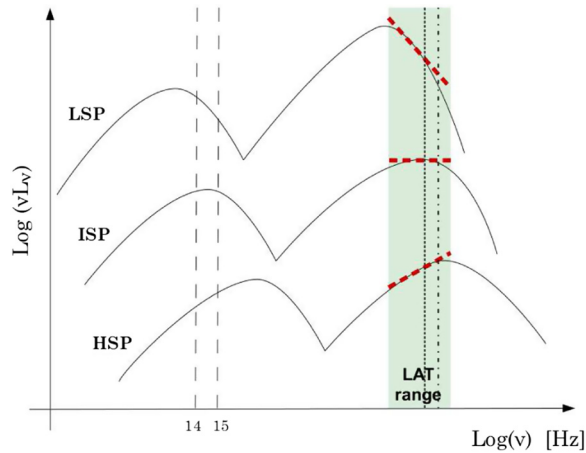
Figure 3. LSP (upper curve), ISP (middle curve) and HSP (lower curve) scchematic SED representation. The 3FGL energy range is represented by the green area, and the black dotted/dash-dotted vertical lines represent the 1FHL/2FHL energy thresholds.

respectively. In the case of LSP blazars both the low- and high-energy SED components peak at lower energies with respect to HSPs, and in general they show softer spectra. By focusing on the high-energy emission SED component, in the case of LSPs within the *Fermi*-LAT energy range (green area in Fig. 3) we are sampling the part of the spectrum where the γ-ray flux is quickly decreasing due to the cooling losses. At $E > 10\,\mathrm{GeV}$, where the radio and γ-ray connection breaks, the steepening is even more pronounced (e.g. Tavecchio & Mazin 2009). On the other hand, in the case of HSP blazars the cooling losses are less severe and their high-energy spectrum peaks at higher energies than LSPs. As a consequence, within the *Fermi*-LAT energy range we are sampling the rising part of the high-energy spectrum, both in the 3FGL and 1-2FHL energy ranges.

This sampling effect, produced by the different SED properties of the different blazar sub-classes, can be related to our correlation results, and can explain why a significant correlation between radio and γ rays at $E > 10\,\mathrm{GeV}$ emission is found only for HSP blazars. Within this simple picture some caveats need to be taken into account (e.g. the variability argument). For the complete correlation analysis, including the 2FHL blazar sample, and the full discussion see Lico *et al.* (2017).

References

Acero, F., Ackermann, M., Ajello, M., *et al.* 2015, *ApJ*, 218, 23

Ackermann, M., Ajello, M., Allafort, A., *et al.* 2011, *ApJ*, 741, 30

Ackermann, M., Ajello, M., Allafort, A., *et al.* 2013, *ApJS*, 209, 34

Ackermann, M., Ajello, M., Atwood, W. B., *et al.* 2016, *ApJS*, 222, 5

Ghirlanda, G., Ghisellini, G., Tavecchio, F., & Foschini, L. 2010, *MNRAS*, 407, 791

Ghisellini, G., & Madau, P. 1996, *MNRAS*, 280, 67

Giroletti, M., Reimer, A., Fuhrmann, L., Pavlidou, V., & Richards, J. L. 2010, arXiv:1001.5123

Kovalev, Y. Y., Aller, H. D., Aller, M. F., *et al.* 2009, *ApJ*, 696, L17

Lico, R., Giroletti, M., Orienti, M., *et al.* 2017, *A&A*, 606, A138

Maraschi, L., Ghisellini, G., & Celotti, A. 1992, *ApJL*, 397, L5

Mufakharov, T., Mingaliev, M., Sotnikova, Y., Naiden, Y., & Erkenov, A. 2015, *MNRA*S, 450, 2658

Pavlidou, V., Richards, J. L., Max-Moerbeck, W., *et al.* 2012, *ApJ*, 751, 149

Piner, B. G., & Edwards, P. G. 2014, *ApJ*, 797, 25

Stickel, M., Padovani, P., Urry, C. M., Fried, J. W., & Kuehr, H. 1991, *ApJ*, 374, 431

Tavecchio, F., & Mazin, D. 2009, *MNRAS*, 392, L40